

Revisiting the alternate load path method for impact-induced progressive collapse in steel moment-resisting frames

Original

Revisiting the alternate load path method for impact-induced progressive collapse in steel moment-resisting frames / Kiakojour, Foad; Zeinali, Elahe; De Biagi, Valerio. - In: INNOVATIVE INFRASTRUCTURE SOLUTIONS. - ISSN 2364-4176. - 10:7(2025), pp. 1-15. [10.1007/s41062-025-02056-0]

Availability:

This version is available at: 11583/3001519 since: 2025-07-03T11:36:50Z

Publisher:

Springer

Published

DOI:10.1007/s41062-025-02056-0

Terms of use:

This article is made available under terms and conditions as specified in the corresponding bibliographic description in the repository

Publisher copyright

(Article begins on next page)



Revisiting the alternate load path method for impact-induced progressive collapse in steel moment-resisting frames

Foad Kiakojouri¹ · Elahe Zeinali¹ · Valerio De Biagi¹

Received: 10 January 2025 / Accepted: 1 May 2025
© The Author(s) 2025

Abstract

Ground-story columns are the most critical and exposed structural members in a frame system. Damage to these members under impact scenarios poses a significant risk to the structure, potentially leading to progressive collapse and severe socio-economic consequences. The predominant approach for assessing structural susceptibility to progressive collapse, both in research and practice, relies on the alternate load path method, which, in its original code-based methodology, follows a threat-independent framework. However, physical collapses are inherently threat-dependent. This study examines the parameters influencing the dynamic response and load-transferring mechanisms of impact-loaded steel moment-resisting frames. Various factors, including the mass and velocity of the impactor, impact height, and impact area, are analyzed and discussed. The findings highlight the differences between dynamic column removal and impact analyses, revealing that, in critical cases, the progressive collapse response can be up to seven times greater than the prediction based on dynamic column removal. This underscores the limitations of the code-based method in high-intensity impact scenarios. Moreover, the overall structural behavior differs, as the effects of initial failure location and energy dissipation patterns vary significantly between the two methodologies. In impact scenarios, at lower intensities, the response is governed by member-level mechanisms, particularly the local response of the column. As intensity increases, system-level performance becomes the dominant factor, reflecting the availability of alternate load paths.

Keywords Impact · Steel moment-resisting frame · Progressive collapse · Load path · Local damage · Extreme event

Introduction

Structural performance under extreme loading conditions has recently gained significant attention, both in research and in practice, due to the increase in natural and anthropogenic hazards [1]. Over the past two decades, a growing number of researchers have focused on the structural robustness and progressive collapse assessment of civil structures and infrastructures. Following the 9/11 events, research has concentrated on one main paradigm: the threat-independent (TI) methodology [2]. In this paradigm, the triggering

event is almost entirely ignored, and member removal policies, mainly static or dynamic column removal, are utilized instead. The alternate load path method has been used in the majority of these threat-independent studies, as well as for design purposes [1, 2].

A code-based, well-established, and well-accepted framework for threat-independent progressive collapse assessment exists today, and the majority of our current understanding of the subject has been achieved through this framework. These studies illuminate the effects of the number of floors [3, 4], seismic design level [3–6], initial failure location [3, 7, 8], different types of irregularities [9–11], and steel connection type [12–14] on the progressive collapse response of frame systems. The obtained results are integrated into modern building codes and ad-hoc guidelines [15–17]. Although most of the literature published on the topic emphasizes the alternate load path method, other techniques such as complexity and compartmentalization have been proposed to enhance and ensure the robustness of civil structures and infrastructure [18].

✉ Foad Kiakojouri
foad.kiakojouri@polito.it
Elahe Zeinali
elahe.zeinali@polito.it
Valerio De Biagi
valerio.debiagi@polito.it

¹ Department of Structural, Geotechnical and Building Engineering (DISEG), Politecnico di Torino, Turin, Italy

As the field matures, an increasing number of threat-dependent (TD) studies are beginning to emerge. These studies, last but not least, challenge some well-known results achieved through threat-independent methodology and shed light on new aspects of the phenomena. Research on blast- [19–22], fire- [23, 24], and impact-induced [25–31] progressive collapse scenarios has led to a paradigm shift in structural robustness and progressive collapse study. These studies have revealed that the structural response in a threat-dependent methodology can differ significantly from those obtained through the threat-independent alternate load path method, both in terms of quantity and quality. This contrast is due to differences in the number of affected members (initial local failure size), the nature of the damage, the time at which damage is applied, and the loading on other members outside the direct damage region [1].

One of the most omnipresent abnormal loading scenarios that can potentially lead to local failure and subsequently total collapse is impact loading on structural columns, which typically occurs at ground level. The source of such impact is usually accidental or intentional car collisions. Rockfall impacts are also frequent phenomena in mountainous areas and highlands. Debris flow [32] and other rare extreme dynamic phenomena can also prompt impact-type loading on structural columns. There is a burgeoning literature on the impact response of steel structures. These studies can be classified into two main groups: those focused on component, member-level, or substructure performance under impact loads, and those devoted to the global response of impact-loaded multi-story, multi-span frames. For the former, a very rich and well-developed literature is already available, in which the impact response of a single member, namely a steel column, is investigated either numerically [33–35] or experimentally [31, 36–38]. In numerical studies, advanced general-purpose finite element packages, namely Abaqus [26, 33, 35], ANSYS [39] or LS-DYNA [25, 34, 40], are usually used. An explicit solver is typically preferred. In experimental setups, a drop hammer [36–38], a pendulum [41], or a pneumatic device [42] is adopted. Referring to the latter, i.e., the impact response of multi-story frames, the literature is limited to a handful of studies. In the numerical studies of impact-loaded steel frames, the impactor is either modeled as a detailed finite element (FE) model, such as a truck [27, 43, 44], a simplified equivalent FE model [26, 27, 45], or as a simple basic geometry [25, 28, 46]. Experimental studies on the impact response of multi-story steel frames are quite rare and usually employ a scaled model [47] to control cost- and space-related issues. There are also a few studies focused on protection measures for structural columns subjected to impact, specifically through the use of energy-absorbing devices [44, 48, 49].

Studies focused on structural performance under extreme loading conditions usually compare the obtained results with

those from threat-independent, code-based static or dynamic column removal methods to highlight the differences. While the studies on the impact response of frame systems are limited in number, the differences between threat-independent and threat-dependent, impact-induced progressive collapse responses are already well-documented [26, 27, 29, 43, 46, 50]. According to the published literature, model structures that meet the code-based criteria for progressive collapse, were severely damaged when subjected to significantly high-speed impacts [43]. At lower impactor velocities, the threat-independent method remains a reliable approach. However, at higher velocities, the progressive collapse potential is significantly greater in the threat-dependent analysis compared to the code-based dynamic column removal method [28]. When impact scenarios are considered, using alternative load path methods to evaluate structural robustness is usually insufficient, as it leads to a structural response significantly different from that obtained through impact analyses [46]. Velocity has a greater influence than mass in increasing the kinetic energy transferred to the building, amplifying vertical vibrations at the node atop the impacted column, and distinguishing between threat-independent and threat-dependent approaches [28]. While impact forces are usually concentrated on a single column (as opposed to blast or fire scenarios where the threat acts on a larger region including several beams, columns, and floor system), dynamic failure of adjacent columns is also observed and reported in numerical modeling [26].

As reviewed, research works that focus on the robustness of impact-loaded steel frame systems are limited in general. Some previous studies have revealed that steel structures act very well under extreme loading conditions; extreme damage, full tearing and complete separation are rare for scenarios such as impact [36–38] or even explosion [51–53]. Such a configuration allows load transferring from the impacted member, namely steel column at ground level, to the main system, and that is, partially explained why the response of the system can exceed those predicted by complete and sudden column removal [21, 29].

This study provides a comprehensive analysis of the dynamic response of impact-loaded steel moment-resisting frames, considering a wide range of influencing parameters. To achieve this, the dynamic responses under various impact scenarios are extracted and compared with one another as well as with the results of dynamic column removal. A parametric study is then conducted to highlight the effects of different parameters, with special emphasis on vertical displacement, energy dissipation, and resistance mechanisms. Several parameters affecting the outcome, related to the impactor (mass, velocity, impact area, and direction) and the frame system (location and height of the impact point), are considered and discussed. This approach is not only beneficial for assessing the structural response of

Table 1 Cross-sections of structural members for steel frame

Story	Column ($B \times B \times t$ mm)	Beam ($h \times b_f \times t_f \times t_w$ mm)		
		NLB	Perimeter-LB	Internal-LB
1	250 × 250 × 16	330 × 160 × 11.5 × 7.5	360 × 170 × 12.7 × 8	400 × 180 × 13.5 × 8.6
2	250 × 250 × 16	330 × 160 × 11.5 × 7.5	360 × 170 × 12.7 × 8	400 × 180 × 13.5 × 8.6
3	250 × 250 × 8	330 × 160 × 11.5 × 7.5	360 × 170 × 12.7 × 8	400 × 180 × 13.5 × 8.6
4	250 × 250 × 8	330 × 160 × 11.5 × 7.5	360 × 170 × 12.7 × 8	400 × 180 × 13.5 × 8.6

impact-loaded frames but also sheds light on the mechanisms of active alternate load paths under extreme loading conditions, providing a solid foundation for understanding the limitations and applicability of the code-based alternate load path method.

Design, modeling and research methodology

Structural response of steel moment-resisting frames subjected to low-velocity impacts was considered and studied herein. Several scenarios that cover a wide range of impact phenomena were contemplated. Since numerical analysis of structures under extreme loading conditions is highly dependent on modeling details and adopted finite element techniques, this section is devoted to such aspects. Details of primary design (Sect. 2.1), finite element modeling techniques (Sect. 2.2), impact loading scenarios (Sect. 2.3), and

code-based column removal method (Sect. 2.4) are provided hereon.

Design of the reference frame structure

The model structure is a 4-story steel moment-resisting frame. The floor height is 3.5 m, thus resulting in a total height of 14 m. The beams span is 5 m in both directions. Side and plan views of the model structure are shown in Fig. 1. The considered dead load and live load are 4.5 and 2 kN/m², respectively. The weight of the exterior wall is considered to be 5 kN/m. All beams and columns are made of St355 steel material. The structural design was performed by means of a commercial package *PRO_SAP*. The gravity and seismic design were performed based on the Italian building code [54]. Considering the structure located in Rome (41.89 N; 12.48 E), the PGA of 0.11 g with the return period of 475 years is adopted for the seismic design [54]. The building is located on Soil type C. While square hollow sections, i.e., box profiles, are used for the columns, I-sections are adopted

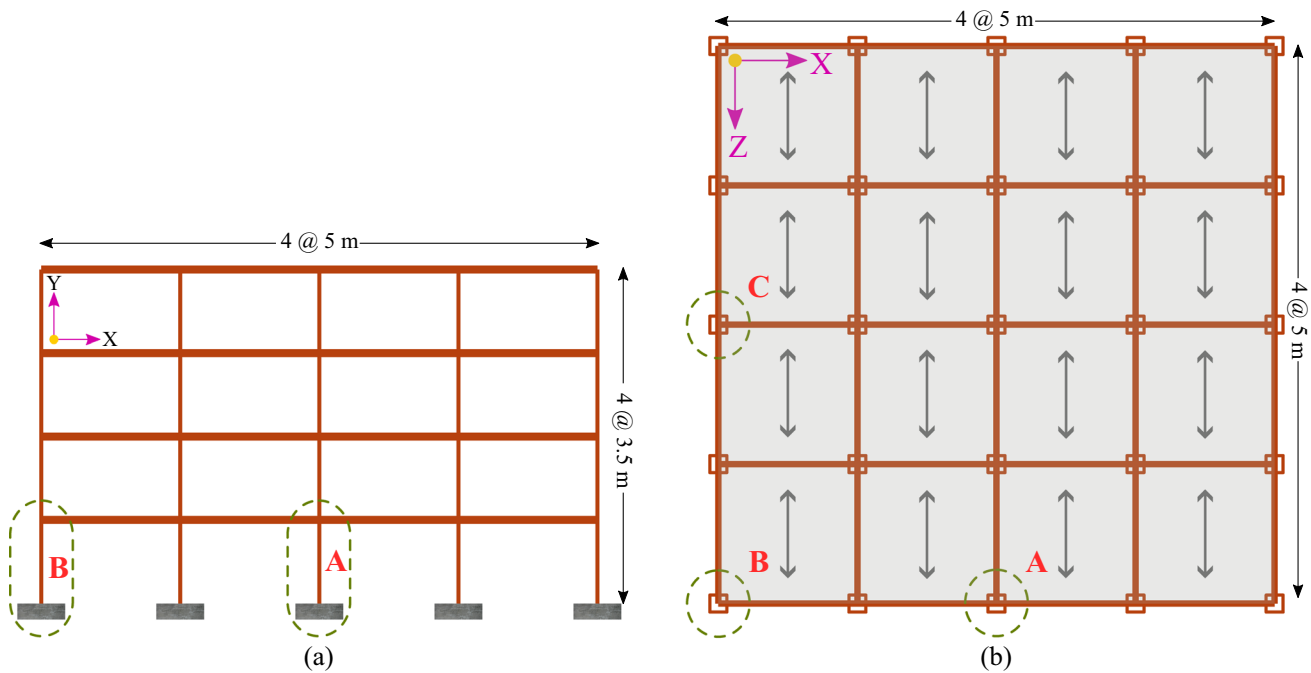


Fig. 1 Model structure and initial failure cases; **a** side view and **b** plan view

for the beams. Considering the utilized one-way slab for the floor system, three beam types are used for load bearing (LB) and non-load bearing (NLB) elements in perimeter and internal frames. Therefore, only the beams in X direction accept the load. Wall loads are applied to perimeter beams in both directions. Two different column cross-sections are employed for the first two stories and second two stories due to member classification policy, that is common in commercial design procedure. The adopted structural sections are listed in Table 1.

Details of finite element modeling

General-purpose finite element software, Abaqus, was employed for the numerical study. The explicit solver was used for impact analyses, while the implicit solver handled dynamic column removal. All beams and columns, except those directly impacted, were modeled using beam elements (B31) from the Abaqus library. Shell elements (S4R) were applied to the impact-loaded columns. S4R, a four-noded reduced-integration shell with hourglass control, has proven effective in previous studies of steel structures subjected to extreme loads [55, 56]. Beam and shell interactions were managed via kinematic coupling to

develop a multi-scale model that simultaneously ensures accuracy and time efficiency. Figure 2 illustrates the multi-scale finite element model.

The significant influence of slabs [57–59] and infills [59–61] on progressive collapse response of frame structures has been emphasized in several recent publications. However, in the current study, these effects are intentionally ignored and shelved for the future. In the first step, for a better understanding of basic load transfer mechanisms and activated alternate load paths in a frame assembly, only the bare frame is under focus. Obviously, more advanced models addressing such details should be developed in future studies, especially if the actual structural response of existing buildings is the main focus.

Three different locations for initial failure in both threat-independent and threat-dependent studies are considered (Cases A–C). These locations are shown in Figs. 1 and 2. It should be noted that using a one-way slab provides a unique opportunity to study similar cases from a structural topology perspective while other parameters differ, which is not possible with two-way slabs. For instance, while the locations of Case A and Case C are similar in terms of global model geometry, the loading scheme and section sizes are different. Therefore, considering both

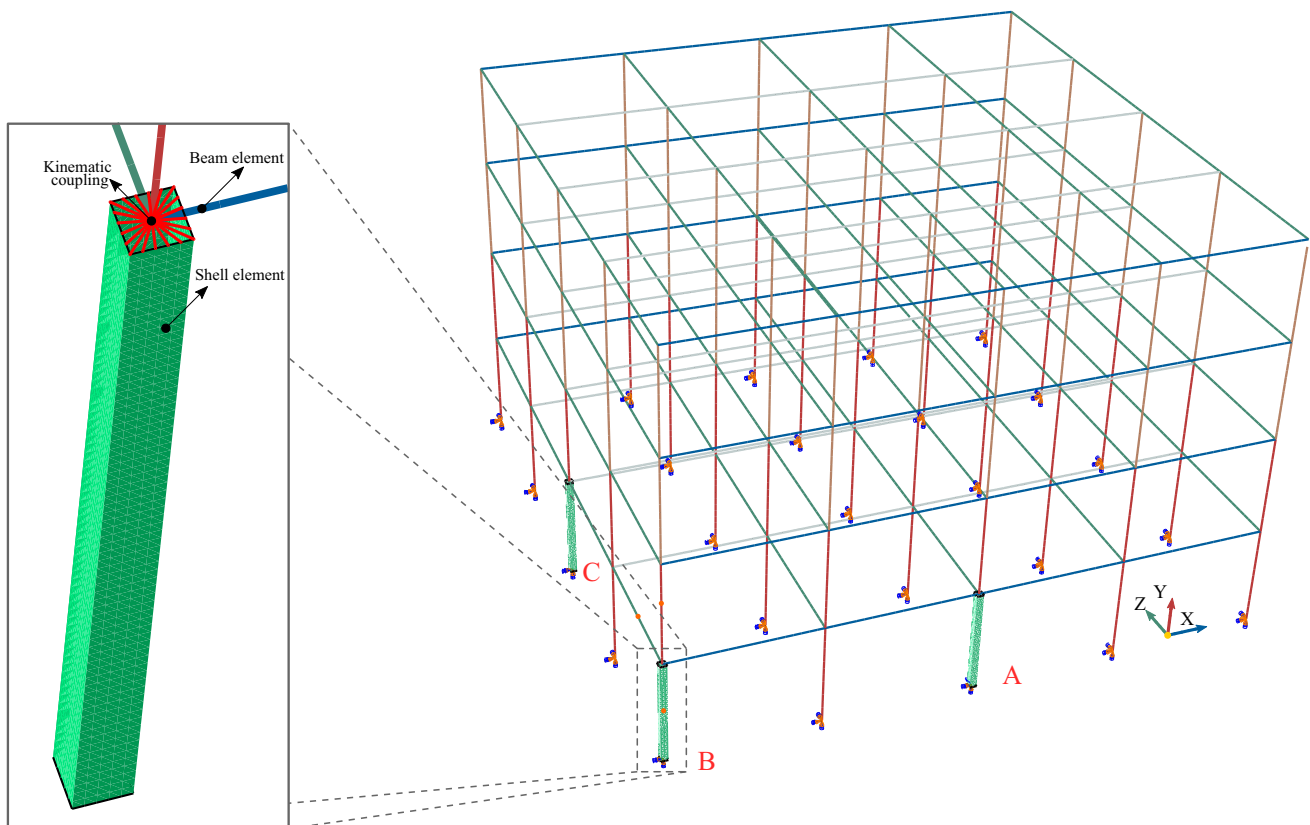


Fig. 2 Details of developed multi-scale finite element model

locations offers better insights into load-bearing mechanisms under impact scenarios.

In modeling the mechanical behavior of steel, the nonlinear part is defined based on the true stress versus logarithmic strain relationship. While post-yield behavior is highly significant under cyclic loading conditions, it can be safely simplified for progressive collapse assessment, particularly when the maximum response is the primary focus [29, 62]. Therefore, in this study, a bilinear elastic–plastic material model was adopted. The Young’s modulus is set to 210 GPa, and the Poisson’s ratio is 0.3. The yield stress and ultimate stress are taken as 355 MPa and 470 MPa, respectively. Isotropic hardening with constant extrapolation is considered. Including more advanced material models and damage parameters is excluded; however, such parameters are important and should be considered when the member-level response is the main research focus.

While strain-rate effects are traditionally ignored in threat-independent progressive collapse assessments, recent studies [62] have shown that they can significantly influence the progressive collapse response. Consequently, strain-rate effects are included in the numerical studies using the Cowper–Symonds equation for both dynamic column removal and impact analyses. The Cowper–Symonds equation is a widely accepted model for characterizing metallic material behavior at high strain rates [21]:

$$\frac{\sigma_{yd}}{\sigma_y} = 1 + \left(\frac{\dot{\epsilon}}{c}\right)^{\frac{1}{q}} \tag{1}$$

where σ_{yd} is the dynamic yield stress, σ_y is quasi-static yield stress, c and q are Cowper–Symonds material constants and $\dot{\epsilon}$ is the strain rate. In the current study $c = 40 \text{ s}^{-1}$ and $q = 5$ were adopted, as suggested for progressive collapse assessment of steel frames in [21, 62]. Damping ratio of 5% of the critical damping is applied, as usually adopted for analysis of structures undergoing extreme loads [3, 62].

Impact scenarios

The structural response to impact loads is influenced by the characteristics of the physical impact. Accordingly, multiple impact scenarios were defined to encompass a reasonable range of mass and velocity. As discussed in Sect. 1, previous studies have often concentrated on threat-specific scenarios, such as truck impacts, with varying levels of simplification. In contrast, this study adopts a generalized approach, focusing on the overall structural response of the impact-loaded frame to simplified impact scenarios, i.e., varying mass and velocity within simple geometries, similar to the methodology reported in [25, 28]. For specific case studies or design purposes, more detailed models should be developed, which are beyond the scope of this study.

For the impact scenarios, gravity loads are initially applied on the frame assembly. To this end, a load combination of $1.2DL + 0.5LL$ (DL and LL stand for dead load and live load, respectively) is adopted. Thenceforward, impact loading is applied to the selected column. Two different weights, 1500 kg and 3000 kg, and three velocities, 10 m/s, 20 m/s, and 30 m/s, are considered for the impact analyses. These conditions result in six impact scenarios with energy levels ranging from 75 to 1350 kJ, where the lower limit corresponds to a 1500 kg impactor at 10 m/s, and the upper limit corresponds to a 3000 kg impactor at 30 m/s. These scenarios are applied to all considered cases, i.e., Cases A–C. While there is no special emphasis on a specific threat, the selected scenarios are in the range of the normal vehicle [26, 28] and/or rockfall [63] impacts and can be considered as representative of these phenomena.

The impactor is modeled as a rigid body with a height of 0.25 m and a length of 0.5 m. The overall configuration is shown in Fig. 3. While deformation and energy dissipation of the impactor can possibly affect the structural response, this effect is ignored in the current study, since the main focus is on the global structural response, not the most accurate modeling of the impact scenario, itself. For contact modeling, the *penalty* method and *hard contact* were selected from the Abaqus library for tangential and normal behaviors, respectively. Separation is allowed after contact. The coefficient of friction was set to 0.3, as recommended in [28, 64, 65].

The impact point is considered in mid-height of the selected columns. In addition to the weight and velocity of the impactor, other parameters including dimensions of the impactor, impact height and direction are also considered for one damage location, i.e., Case B.

Dynamic column removal scenarios

Dynamic column removal analyses were performed to provide a basis for comparison of impact-loaded frames with the code-based threat-independent approach. For dynamic column removal, a three-step methodology, as described in Fig. 4, is adopted. Initially, in Step 1, gravity loads were statically applied on the intact structural assembly. The applied load combination is similar to what described in Sect. 2.3 for impact analyses. In Step 2, that is dynamic, “**model change, remove*” command from the Abaqus library is utilized for sudden column removal. Column removal cases, that are similar to those accepting the impact loads in the previous analyses, are shown in Fig. 1. In Step 3, the free vibration is monitored. An implicit solver was used in this methodology, since “**remove*” command is only available in this solver. Such a methodology is widely adopted in threat-independent progressive collapse studies of frame systems [62]. Otherwise, more time-consuming approaches, i.e.,

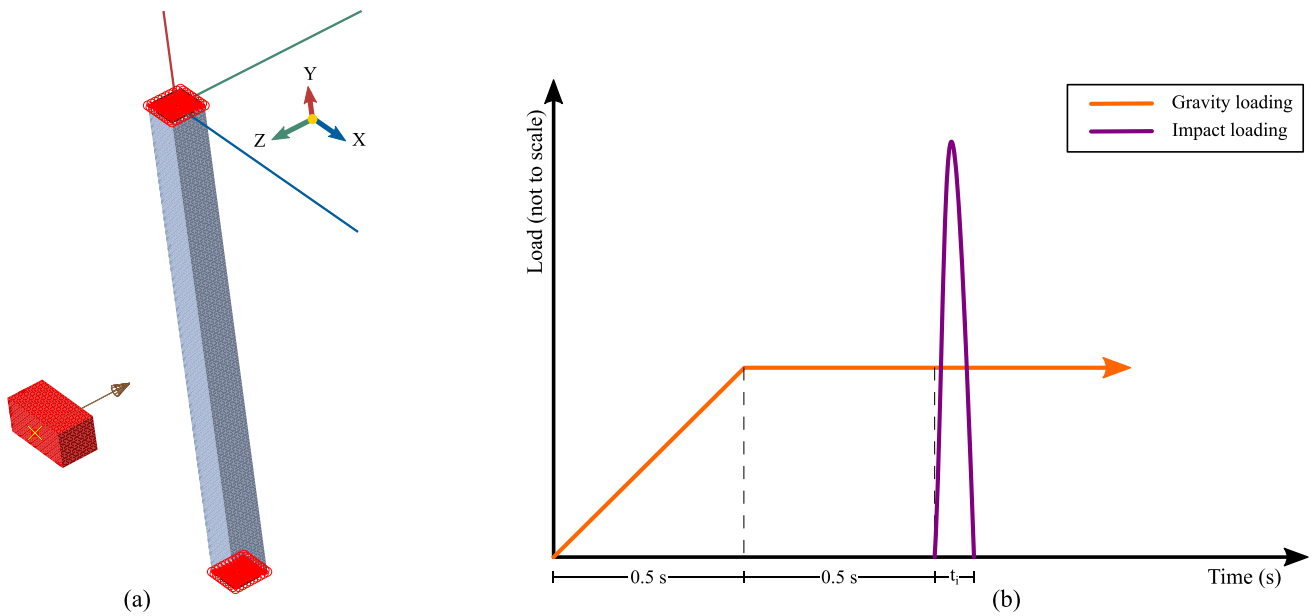


Fig. 3 Impact loading on the column and details of the impact scenarios: **a** multi-scale model integrating beam and shell elements, and **b** gravitational and impact loading sequence

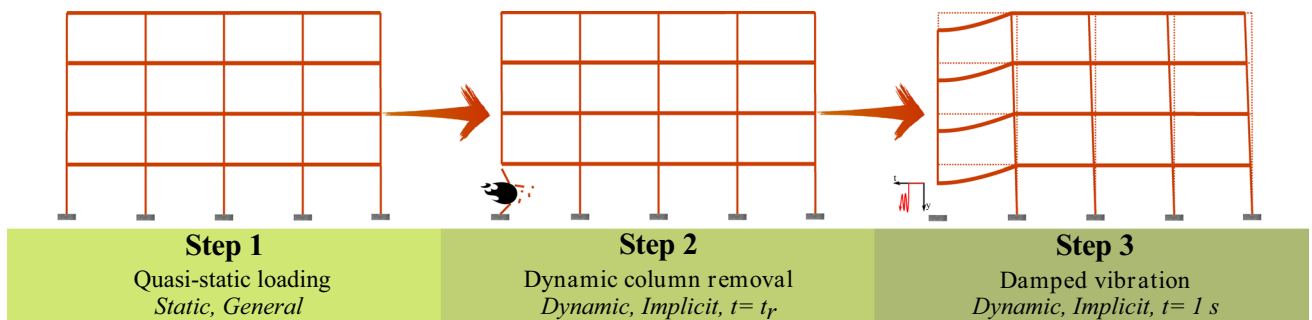


Fig. 4 Procedure for dynamic column removal analysis

so-called force-based column removal approach [3] should be utilized. Column removal time, i.e., t_r in Fig. 4, is set to 1 millisecond, with a monitoring period of 1 s after removal. The rationale for this selection is discussed in [62, 66].

Summary of performed analyses

In progressive collapse studies, two classes of analytical approaches exist. The first is the threat-dependent approach, in which the acting threat is directly modeled. The second, referred to as the threat-independent approach, involves sudden column removal analysis, where the selected column is dynamically removed from the structural assembly. Within this framework, two sets of numerical analyses were conducted to achieve the objectives of this study. The first set consists of threat-dependent impact-induced progressive collapse analyses, followed by parametric analyses considering

various factors such as impactor speed, mass, impact area, and impact height. The second set includes threat-independent dynamic column removal analyses, primarily used for comparison. Analysis details and numerical techniques for the former, i.e., *threat-dependent* impact-induced progressive collapse, and the latter, i.e., *threat-independent* dynamic column removal, were provided in Sect. 2.3 and Sect. 2.4, respectively. These two analysis sets are applied to similar initial failure locations, as described in Figs. 1 and 2. Table 2 summarizes the impact analyses and adopted parameters.

Verification of the finite element model

Dynamic full-scale progressive collapse tests are quite scarce, and threat-dependent tests for the progressive collapse of steel frames under impact are even more limited.

Table 2 Summary of performed analyses

Location	Velocity (m/s)	Weight (kg×10 ³)	Direction	Impact height (m)	Impact area (m ²)
A	10, 20 and 30	1.5 and 3	Z	1.75	0.25 × 0.25
B	10, 20 and 30	1.5 and 3	X and Z	0.875, 1.75 and 2.625	0.25 × 0.25, 0.25 × 0.5 and 0.25 × 0.75
C	10, 20 and 30	1.5 and 3	X	1.75	0.25 × 0.25

Therefore, full validation of the type of simulation reported in the current study is challenging. However, the overall finite element techniques and adopted methods have been examined using experimental data from member-level impact tests reported in [67] for partial validation of the numerical model. The verified model structures are hollow tubes under low-velocity lateral impact (4.427 m/s). Among the reported test specimens, two models, i.e., T3 and T6, were adopted for verification. While the diameter, thickness and effective length for the model T3 are 31.8, 1.75 and 480 mm, these values for the model T6 are 38.1, 1.90 and 640 mm, respectively. The weight of the impactor for model T3 is 99.4 kg, while for the Model T6 the weight is 72.0 kg. The yield stress of the tubes used in the experiment is approximately 1300 MPa, and the Young’s modulus is set at 206 GPa. The impact tests were conducted using a hammer impact machine. The rigid impactor had a round arc surface with a diameter of 30 mm, a central angle of 160°, and a width of 80 mm. More details can be found in [67]. The fundamental numerical modeling techniques

are similar to those described in Sect. 2 for the core of the paper. In extreme loading scenarios such as blast and impact, the focus is primarily on predicting the maximum response, which typically occurs during or immediately after loading. Therefore, the simulation time was limited to capturing the peak response values. Figure 5 shows a comparison between the results of above-stated tests and the performed numerical studies. The results are within the acceptable range especially referring to the maximum displacement.

Results and discussions

The results of threat-independent, code-based dynamic column removal and threat-dependent impact-induced progressive collapse analyses are presented and discussed herein. The term *response* refers to the vertical displacement at the column removal point (CRP) unless otherwise specified. The CRP corresponds to the top node of the removed column in dynamic column removal analyses or the top node of the

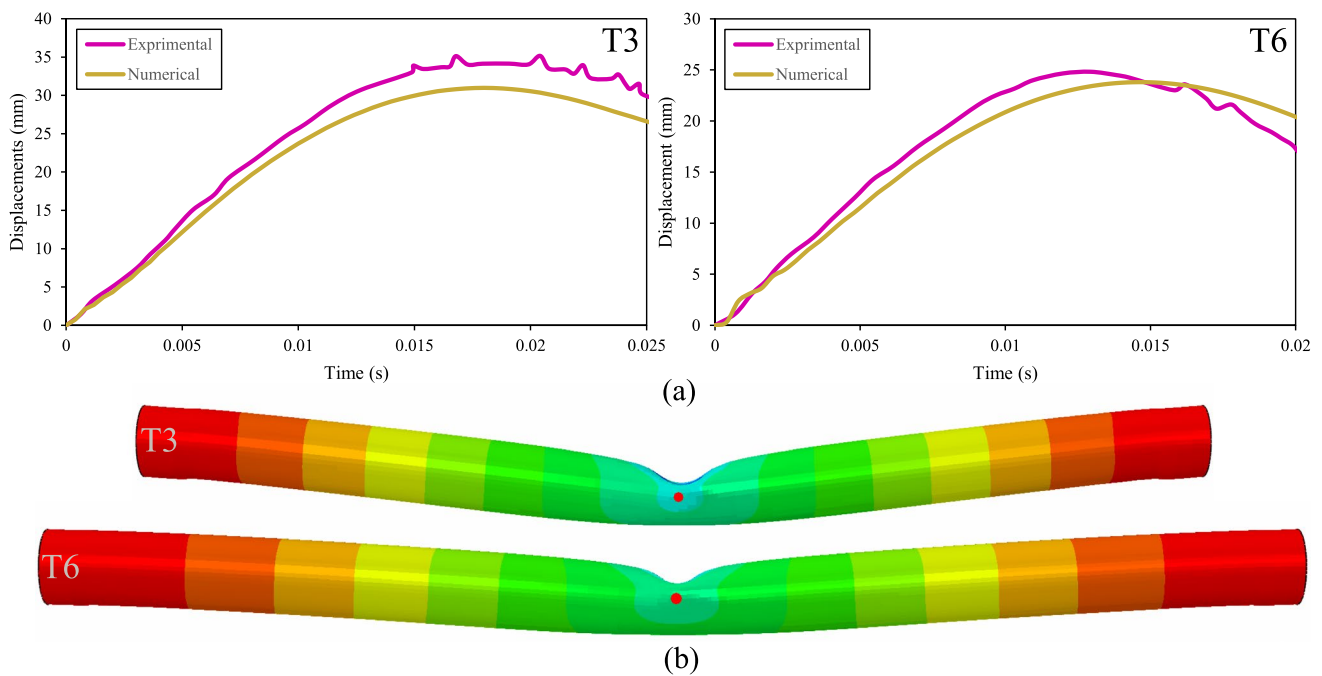


Fig. 5 Comparison of numerical and experimental results; **a** time-histories of displacements and **b** deformed shapes

damaged column in impact analyses. All horizontal displacements are monitored and reported at impact height levels, whether they occur at mid-height, one-third, or two-thirds of the column height.

Dynamic response under impact scenarios

As anticipated from the fundamental equations, the impact response of the model structure is highly influenced by the velocity and mass of the impactor, with the former exerting a significantly greater effect. Figure 6 illustrates the displacement time-history for various cases, all characterized by the impact at column mid-height (1.75 m) and equal impact area of 0.25×0.25 m², while Table 3 presents the maximum displacement for the mentioned scenarios. In this table, TI represents the maximum response from threat-independent column removal analyses for comparison. It should be noted that all the observed maximum values for beams in

threat-independent column removal analyses comply with the rotation limitations recommended by the GSA guidelines [3, 16]. Interestingly, the same observation applies to threat-dependent impact scenarios, as the beam chord rotation remains within the allowable limit in all examined cases.

It was observed that at lower velocities (e.g., 10 m/s), Case A results in greater displacement, making it the critical case. However, as impact intensity increases with velocity, the critical location shifts to Case B. This shift can be attributed to the structural configuration and loading scheme. At lower intensities, the response is governed by member-level mechanisms, making Case A more critical due to higher gravitational loads. As intensity increases, system-level performance becomes the dominant factor, making Case B more critical due to the limited availability of alternate load paths compared to Case A.

Comparing the influence of impact direction in Case B, the differences were minimal, and no significant variations

Table 3 Maximum vertical displacements in millimeters for threat-independent (dynamic column removal) and threat-dependent (impact analysis) scenarios

	1500			3000			TI
	Weight (kg)	Velocity (m/s)		Weight (kg)	Velocity (m/s)		
Case A	2.5	10	20	5.8	20	30	33.4
Case BX	2	10	20	5	20	30	37.5
Case BZ	2	10	20	4.9	20	30	37.5
Case C	1.9	10	20	5.1	20	30	21

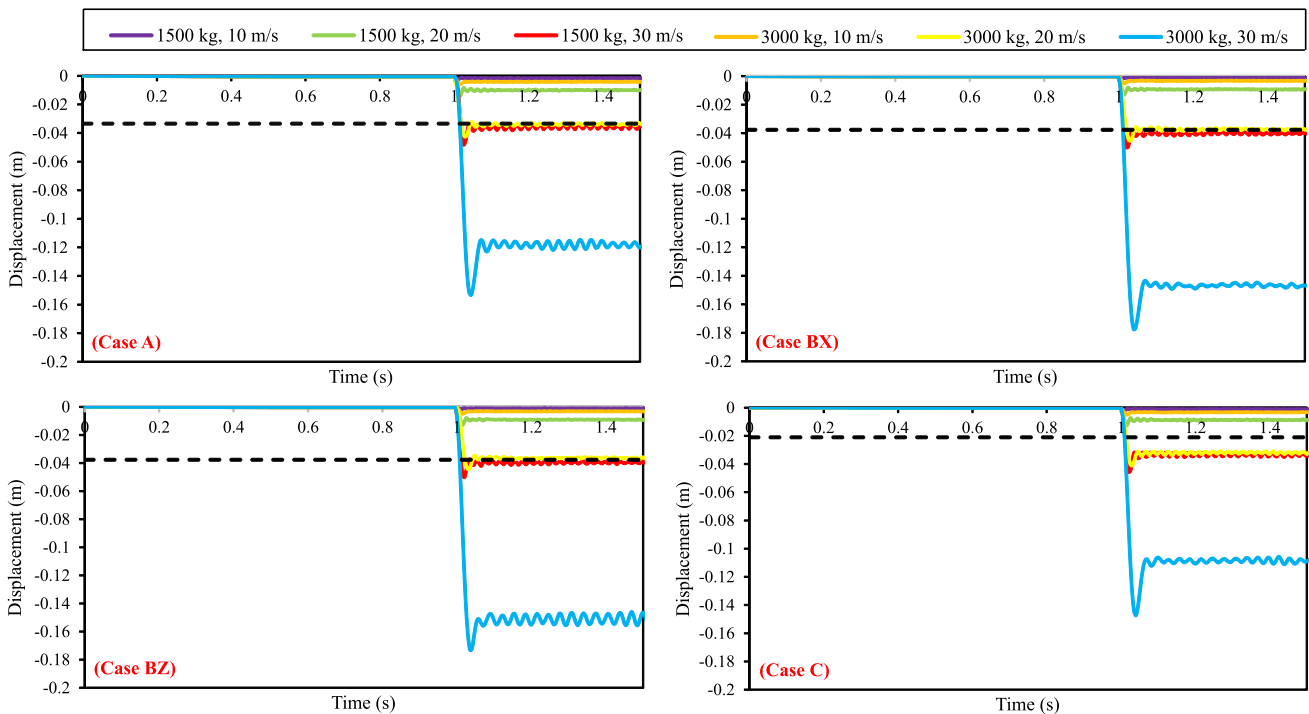


Fig. 6 Vertical displacement under different impact scenarios. The dashed line illustrates the associated maximum displacement in dynamic column removal

were observed, except for the highest intensity (3000 kg at 30 m/s), where Case BX was slightly more critical compared to Case BZ. This behavior can be attributed to the fact that the primary frames are arranged along the X direction. This means that the inertia of the masses along the X direction is greater than along the Z direction because the floor masses are supported by the primary frames. At the same time, the primary frame (along the X direction) is stiffer towards horizontal forces than the secondary frame (along the Z direction). Considering that the higher the inertia and stiffness, the greater the collision force, an impact along the X direction causes a greater force and thus causes greater damage to the component than an impact along the Z direction. This emerges when the effects turn from local (member level) to global (system level), hence at high kinetic energies.

It is interesting to note that the effect is not solely proportional to the kinetic energy but also depends on the weight of the impacting mass, even at low kinetic energies. For example, although a 1500 kg mass at 10 m/s has half the kinetic energy of a 3000 kg mass at 10 m/s, the displacement in the latter case is more than twice that of the former. This is because the collision force is influenced by the ratio between the masses of the impactor and the impacted member, as illustrated by [68].

The results of the threat-independent study, i.e., the time-histories of vertical displacements in dynamic column removal scenarios, are presented in Fig. 7, following the methodology explained in Sect. 2.4. The maximum vertical displacements extracted from the time-history curves for the three dynamic column removal cases are highlighted in Table 3. It should be noted that within the threat-independent framework, Cases BX and BZ are identical. These maximum vertical displacements are indicated by a horizontal dashed line in Fig. 6 to serve as a basis for comparison with impact scenarios. As clearly observed in the results, the maximum response of the impact-loaded structure can significantly exceed that observed in the dynamic column removal. For

a 1500 kg impactor at a velocity of 30 m/s (having a kinetic energy of 675 kJ), and a 3000 kg impactor at a velocity of 20 m/s (having a kinetic energy of 600 kJ), the maximum response moderately exceeds the dynamic column removal response for all considered cases. However, for the 3000 kg impactor at 30 m/s (having a kinetic energy of 1350 kJ), the response far exceeds the threat-independent response. In the most critical case, Case C, the impact response is seven times higher than the column removal response. This difference arises from several factors. It should be noted that code-based dynamic column removal results in the clean and complete removal of the member from the structural assembly, without causing additional damage or loading to other members. In contrast, in an impact-loaded structure, extra load is applied to the system, which can lead to increased displacement or even damage.

Figure 8 presents the deformed shape of the damaged column under various impact scenarios, with the maximum horizontal displacement indicated in the legend. All cases involve a 25x25 cm² impactor striking the column at its mid-height. To better visualize the deformation, the column is sectioned at the impact center. Such deformation applies an extreme load to the CRP. As analytically investigated and reported in [29], a damaged but still connected member can transfer extreme loads to the structure through a vertical catenary mechanism. This explains why the response in a damaged assembly can exceed the response in a system with complete sudden column removal. Interestingly, similar results have also been reported for reinforced concrete frames subjected to impact scenarios, where the downward force exerted by the impacted columns is a significant contributing factor to progressive collapse performance [69].

It should be noted that this observation is not directly and entirely governed by the damage level in the column. As observed, no progressive collapse occurs even in the case of sudden and complete column removal (i.e., 100% damage level). Therefore, in a threat-independent framework, lower damage levels would also not be expected to cause collapse. On the other hand, as explained, in certain threat-dependent impact-induced scenarios, specifically, the three scenarios with kinetic energy equal to or exceeding 600 kJ, the response surpasses that of dynamic column removal. This is not directly related to the residual capacity of the column itself but rather to its role as a mediating element that transfers extreme loads to the main frame, resulting in additional vertical deformation, even compared to complete sudden column removal. Overall, structural response and progressive collapse performance are not directly dictated by the damage level in the impacted column. Instead, performance is primarily governed by the capacity of the main structural frame to provide alternative load paths following initial damage, as well as by the ability of the impacted column to transfer extreme loads to the main structure. While

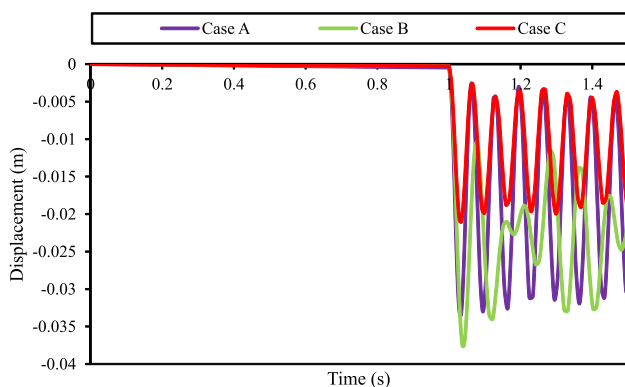


Fig. 7 Vertical displacement under threat-independent dynamic column removal scenarios

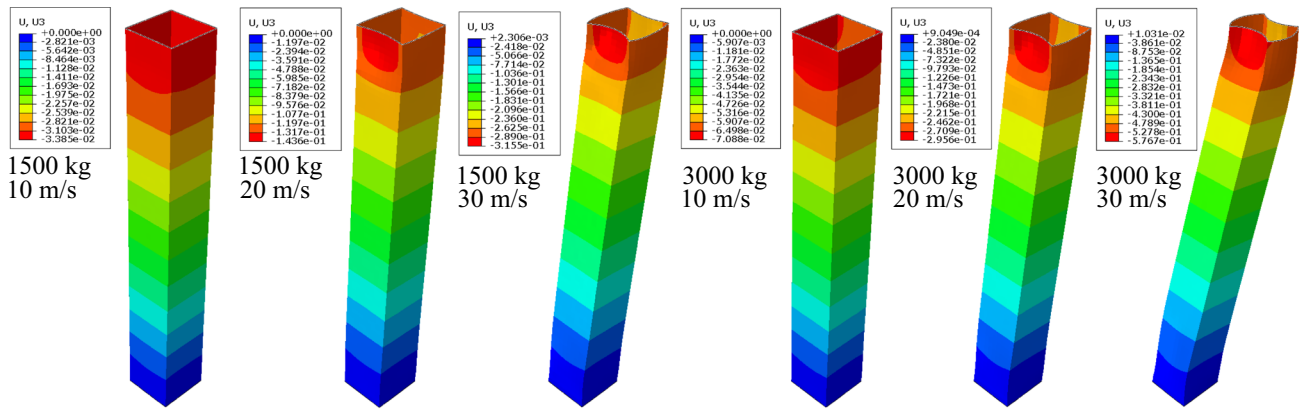


Fig. 8 Cross-section of the deformed shapes of the (half) column under different impact scenarios ($25 \times 25 \text{ cm}^2$). The columns are cut at the impact level (mid-height) for better presentation. The legend illustrates the horizontal displacement

the latter is indirectly influenced by the damage state of the column, this effect is significant mainly before reaching maximum damage levels.

Referring to the impact location, a well-known and predictable pattern is observed in threat-independent column removal scenarios. Specifically, the most critical scenario is Case B, the corner column removal scenario. Comparing the two other cases, Case A and Case C, less vertical displacement is observed in Case C, simply because in this case the beams above the removed column carry less load. All of these observations can be interpreted based on system-level performance. Case B represents a corner column removal scenario, where, considering the structural topology, fewer members participate in load-bearing after column removal compared to the other two cases. In other words, fewer alternative load paths are available, which clearly explains the observed results. On the other hand, in the impact scenarios, both system-level performance (referring to the alternate load paths in the frame system) and member-level performance (referring to the impacted column itself) are equally important. As shown in Table 3, in several impact scenarios, Case A is the most critical. This is because, in these cases, member-level performance dominates the overall dynamic response.

The results also highlight the differences in member participation between threat-independent column removal and threat-dependent impact analyses. In dynamic column removal, the beams directly connected to the removed column serve as the primary resisting members, while the columns above the removed column do not directly contribute to the resisting mechanism. In contrast, in impact analyses, the impacted column plays a crucial role in structural robustness assessment. This is not only due to its significant contribution to energy dissipation but also because it serves as a mediating element, transferring the extreme load to the main structural system.

Figure 9 illustrates the participation of structural members in energy dissipation under two impact scenarios. These members are indicated in Fig. 2 with an orange circle for better visualization. It should be noted that similar trends are observed for other scenarios. In all cases, most of the plastic energy dissipation occurs in the impacted column, and as the impact intensity increases, the share of the impacted column decreases, indicating that other members begin to dissipate energy through plastic deformation. In Fig. 9a, the plastic dissipation in the connected beam in the impact direction and the top column are nearly equal, while in Fig. 9b, which represents a more intense impact scenario, the dissipation in the beam surpasses all other members except the impacted body. These observations should be interpreted in the context of the presence of extreme horizontal forces, which explain why the top column also participates in energy dissipation, in contrast to dynamic column removal, where mainly beams are involved.

Parametric analyses

Analysis cases considering impact height and impacted area are presented in Table 2. For the impacted area, three scenarios are examined, with the corresponding results shown in Figs. 10 and 11. To better understand the physical phenomenon, both the vertical displacement at the top node of the damaged column and the horizontal displacement at the column's mid-height, i.e., impact level, are monitored and reported. As expected, an increase in the impacted area results in decreased horizontal and vertical displacements. This occurs because a more concentrated force leads to localized plastic deformation, which influences both the member-level response (horizontal displacement) and the system-level response (vertical displacement). In general, horizontal displacements are observed to be three to five times larger than vertical displacements.

Fig. 9 Plastic dissipation distribution in structural members in Case BZ: (a) impact scenario with a 1500 kg impactor at 30 m/s, and (b) impact scenario with a 3000 kg impactor at 30 m/s

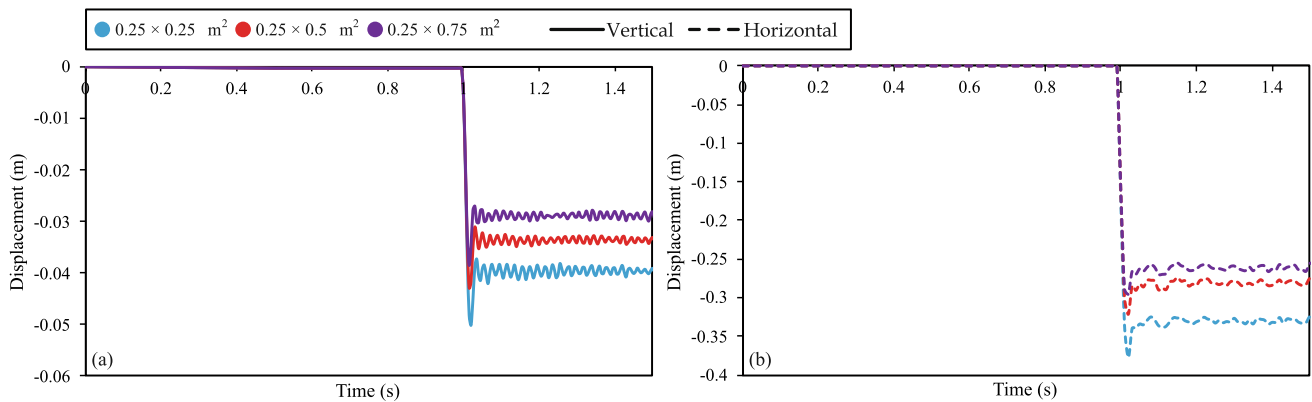
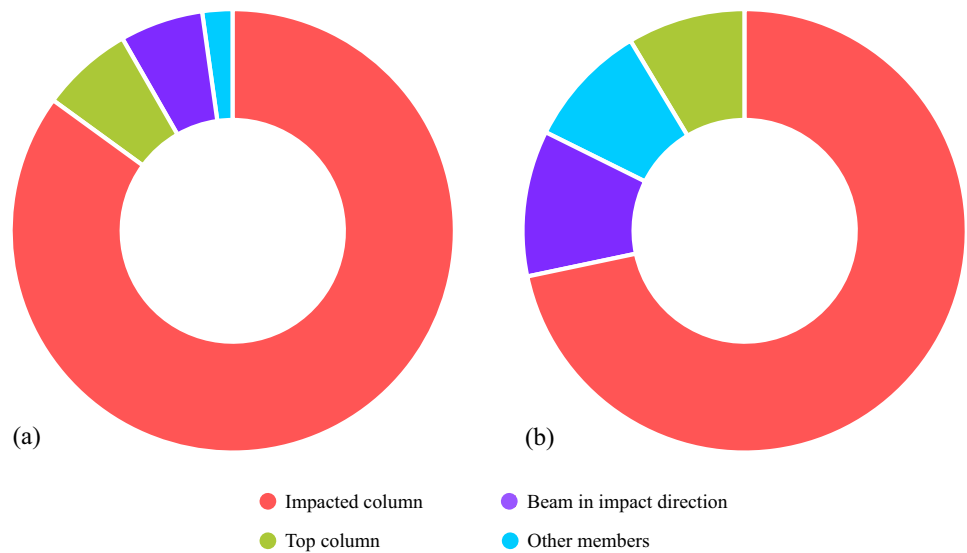


Fig. 10 Case BZ subjected to an impact of 1500 kg at 30 m/s; **a** vertical displacement in top node of damaged column and **b** horizontal displacement under impact center in column mid-height

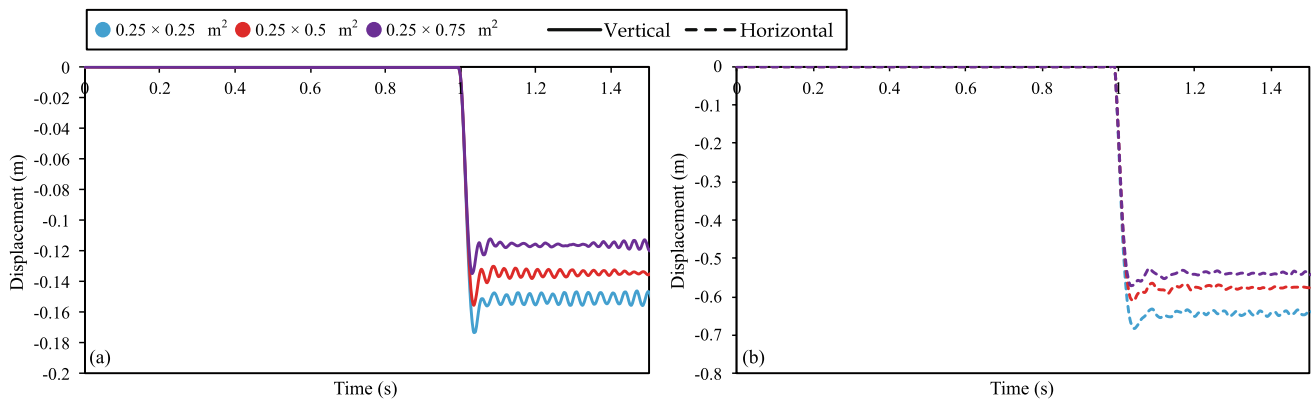


Fig. 11 Case BZ subjected to an impact of 3000 kg at 30 m/s; **a** vertical displacement in top node of damaged column and **b** horizontal displacement under impact center in column mid-height

Figure 12 shows the vertical displacements at the damaged column's top node for two selected impact scenarios (BZ) at three different heights: 0.875, 1.75, and 2.625 m. As mentioned in Sect. 2, this study does not aim to provide a detailed realistic impact scenario or a specific case study. However, the chosen heights can be justified in the context of car impacts, where there is a difference in the level of the street and the building's story levels in car collision scenarios, or in rockfall impacts, where the impact can occur at any point on the column. As anticipated and clearly shown in Fig. 12, impact at the column's mid-height leads to the most critical scenario. Comparing the two other cases, an impact position closer to the top of the column results in a less critical scenario compared to the location near the column base.

Conclusions and future research directions

To verify the application of the alternate load path method and understand its limitations, it is crucial to focus more on a threat-dependent methodology. The current study is devoted to this purpose, focusing on the parameters affecting the dynamic response and load transferring mechanisms of an impact-loaded steel moment-resisting frame. The differences in structural responses between threat-independent method, i.e., dynamic column removal, and threat-dependent method, i.e., impact analysis, are highlighted.

By increasing the impact energy 18 times (comparing the lightest impactor at the lowest velocity to the heaviest impactor at the highest velocity), the maximum responses increase by 61 to 88 times, depending on the damage location. Therefore, development and application of the non-structural measures, that can stop the impactor or decrease its velocity efficiently, are of great importance to control the initial damage size and intensity. For the vehicle impact, bollards and different energy dissipation systems, i.e., sandwich structures, are currently being used by engineers. For other

possible impact scenarios more emphasis is vital to develop efficient devices and techniques.

The obtained results clearly highlight the differences between dynamic column removal and impact analyses. In many cases, the progressive collapse potential significantly exceeds the prediction of dynamic column removal, emphasizing the limitations of the code-based method in intense impact scenarios. In the most critical case, the impact response from the threat-dependent study is seven times higher than that of the threat-independent column removal analysis. It should also be noted that the difference between threat-independent and threat-dependent methods is not limited to the extent of the displacement; the overall behavior can also differ. For example, the effect of the initial local failure is not always the same in the two methodologies. The paper also studied the parameters affecting the impact response and further confirms that increasing the impacted area leads to a decrease in vertical displacement. By increasing the impact area three times, the vertical displacements at the column top node decrease by approximately 22–24% for different impact energies. Additionally, the most critical impact point is at the mid-height of the column, where the responses decrease by 15–56% in cases where the impact point is considered one third and two thirds of the column height, across different scenarios.

Threat-dependent progressive collapse study is a young field in the structural engineering realm. Among the different branches of this field, impact-induced progressive collapse has received less research focus, and therefore, a lot of research potential can be found. The global impact response of different frame systems, namely various types of braced frames, needs much more research focus. Performance of different steel connections subjected to impact loads at the member level is already highlighted. However, the effects of different steel connections in energy dissipation and load transferring mechanisms at system level require special attention. Moreover, in the current limited literature,

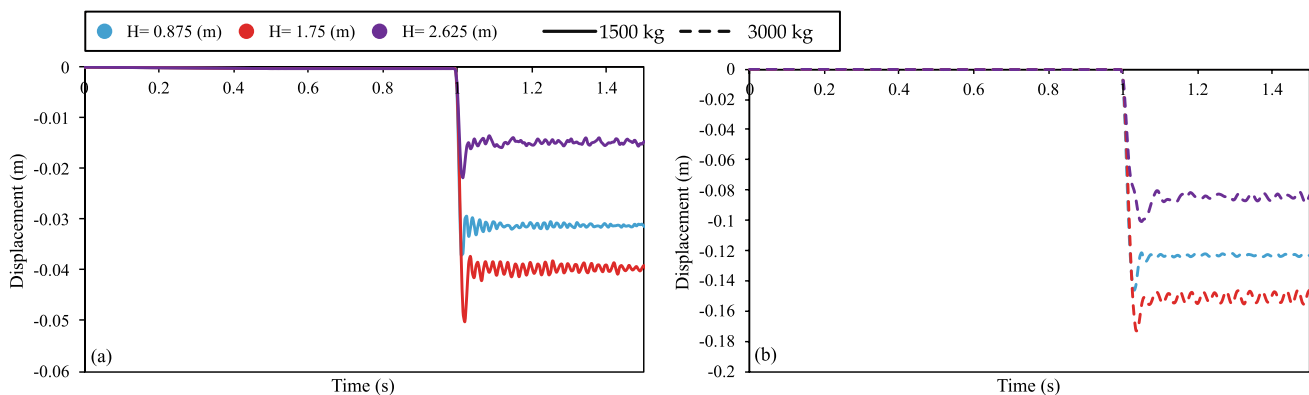


Fig. 12 Case BZ subjected to impact scenarios at 30 m/s from different heights: **a** vertical displacement time histories for a 1500 kg impactor, and **b** vertical displacement time histories for a 3000 kg impactor

the impactor, explicitly or implicitly (different equivalent and simplified models), represents a vehicle. More research focus is still needed on the other possible scenarios, i.e., rockfall, debris and flow impact on the frame assemblies. Into the bargain, more research emphasis should be placed on repeated impacts, on the same or different column, and multiple impacts on a single column, since the body of the current literature is mainly limited to single impact scenarios.

Acknowledgements This study is part of the project NODES which has received funding from the Italian Ministry of University and Research (MUR) - M4C2 1.5 of PNRR funded by the European Union - NextGenerationEU (Grant agreement no. ECS00000036).

Funding This study was carried out within the project "A Quantitative Framework for Structural Robustness Assessment" (CUP E53C24002780006), funded by the Italian Ministry of University and Research under the PRIN 2022 program (D.D. 104 - 02/02/2022), and the NODES project, which has received funding from the Italian Ministry of University and Research (MUR) - M4C2 1.5 of PNRR, funded by the European Union - NextGenerationEU (Grant Agreement No. ECS00000036). This manuscript reflects only the authors' views and opinions; the Ministry cannot be held responsible for them.

Declarations

Conflict of interest The authors declare that they have no known competing financial interests or personal relationships that could have appeared to influence the work reported in this paper.

Open Access This article is licensed under a Creative Commons Attribution-NonCommercial-NoDerivatives 4.0 International License, which permits any non-commercial use, sharing, distribution and reproduction in any medium or format, as long as you give appropriate credit to the original author(s) and the source, provide a link to the Creative Commons licence, and indicate if you modified the licensed material. You do not have permission under this licence to share adapted material derived from this article or parts of it. The images or other third party material in this article are included in the article's Creative Commons licence, unless indicated otherwise in a credit line to the material. If material is not included in the article's Creative Commons licence and your intended use is not permitted by statutory regulation or exceeds the permitted use, you will need to obtain permission directly from the copyright holder. To view a copy of this licence, visit <http://creativecommons.org/licenses/by-nc-nd/4.0/>.

References

- Kiakojoury F, Sheidaii MR, De Biagi V, Chiaia B (2021) Progressive collapse of structures: a discussion on annotated nomenclature. *Structures* 29:1417–1423. <https://doi.org/10.1016/j.istruc.2020.12.006>
- Kiakojoury F, De Biagi V, Marchelli M, Chiaia B (2024) A conceptual note on the definition of initial failure in progressive collapse scenarios. *Structures* 60:105921. <https://doi.org/10.1016/j.istruc.2024.105921>
- Kim J, Kim T (2009) Assessment of progressive collapse-resisting capacity of steel moment frames. *J Constr Steel Res* 65(1):169–179. <https://doi.org/10.1016/j.jcsr.2008.03.020>
- Kordbagh B, Mohammadi M (2017) Influence of seismicity level and height of the building on progressive collapse resistance of steel frames. *Struct Des Tall Spec Build* 26(2):1305. <https://doi.org/10.1002/tal.1305>
- Rezvani FH, Asgarian B (2014) Effect of seismic design level on safety against progressive collapse of concentrically braced frames. *Steel Compos Struct Int J* 16(2):135–156. <https://doi.org/10.12989/scs.2014.16.2.135>
- Sheikh TA, Banday J, Pasupuleti VDK (2024) Percentile influence of beam column cross-sectional design on progressive collapse potential of low-rise reinforced concrete framed structure. *Innov Infrastruct Solut* 9(2):40. <https://doi.org/10.1007/s41062-023-01349-6>
- Fu F (2009) Progressive collapse analysis of high-rise building with 3-d finite element modeling method. *J Constr Steel Res* 65(6):1269–1278. <https://doi.org/10.1016/j.jcsr.2009.02.001>
- Biagi VD, Kiakojoury F, Chiaia B, Sheidaii MR (2020) A simplified method for assessing the response of rc frame structures to sudden column removal. *Appl Sci* 10(9):3081. <https://doi.org/10.3390/app10093081>
- Raikar RG, Kangda MZ (2023) Effect of plan irregularity on the performance of steel buildings subjected to blast-induced vibrations. *Innov Infrastruct Solut* 8(2):77. <https://doi.org/10.1007/s41062-023-01034-8>
- Ebadi-Jamkhaneh M, Kontoni D-PN, Homaioon Ebrahimi A (2024) Assessment of different methods for enhancing progressive collapse resistance of irregular reinforced concrete buildings using pushdown analysis. *Arab J Sci Eng* 11:1–23. <https://doi.org/10.1007/s13369-024-08847-4>
- Singh H, Tiwary AK (2025) Evaluating progressive collapse performance of structures containing plan irregularities: a comparative analysis of column elimination scenarios. *Structures* 72:108239. <https://doi.org/10.1016/j.istruc.2025.108239>
- Kim T, Kim J (2009) Collapse analysis of steel moment frames with various seismic connections. *J Constr Steel Res* 65(6):1316–1322. <https://doi.org/10.1016/j.jcsr.2008.11.006>
- Chen C, Qiao H, Wang J, Chen Y (2020) Progressive collapse behavior of joints in steel moment frames involving reduced beam section. *Eng Struct* 225:111297. <https://doi.org/10.1016/j.engstruct.2020.111297>
- Salmasi A, Sheidaii MR, Tariverdilo S (2021) Performance of fully restrained welded beam-column connections subjected to column loss. *Int J Steel Struct* 21(4):1370–1382. <https://doi.org/10.1007/s13296-021-00505-x>
- DoD (2009) Design of buildings to resist progressive collapse, Unified Facilities Criteria (UFC) 4-023-03. Department of Defense, Washington, DC
- GSA (2016) Progressive collapse analysis and design guide lines for new federal office buildings and major modernization project, Washington, DC
- Agrawal A, Ettouney M, Chen X, Li H, Wang H et al (2020) Steel truss retrofits to provide alternate load paths for cut, damaged, or destroyed members (fhwa-hrt-20-055). United States. Federal Highway Administration, Technical report
- Kiakojoury F, De Biagi V, Abbracciavento L (2023) Design for robustness: bio-inspired perspectives in structural engineering. *Biomimetics* 8(1):95. <https://doi.org/10.3390/biomimetics801095>
- Pourasil MB, Mohammadi Y, Gholizad A (2017) A proposed procedure for progressive collapse analysis of common steel building structures to blast loading. *KSCE J Civ Eng* 21(6):2186–2194. <https://doi.org/10.1007/s12205-017-0559-0>
- Gombeda MJ, Naito CJ, Quiel SE, Fallon CT (2017) Blast-induced damage mapping framework for use in threat-dependent progressive collapse assessment of building frames. *J Perform*

- Constr Fac 31(2):04016089. [https://doi.org/10.1061/\(ASCE\)CF.1943-5509.0000949](https://doi.org/10.1061/(ASCE)CF.1943-5509.0000949)
21. Kiakojouri F, Sheidaii MR, De Biagi V, Chiaia B (2021) Blast-induced progressive collapse of steel moment-resisting frames: numerical studies and a framework for updating the alternate load path method. *Eng Struct* 242:112541. <https://doi.org/10.1016/j.engstruct.2021.112541>
 22. Ambavaram VS, Muddarangappagari A, Mekala A, Chenna R (2021) Dynamic performance of multi-Storey buildings under surface blast: a case study. *Innov Infrastruct Solut* 6(4):223. <https://doi.org/10.1007/s41062-021-00585-y>
 23. Sun R, Huang Z, Burgess IW (2012) Progressive collapse analysis of steel structures under fire conditions. *Eng Struct* 34:400–413. <https://doi.org/10.1016/j.engstruct.2011.10.009>
 24. Shan S, Li S (2020) Fire-induced progressive collapse mechanisms of steel frames with partial infill walls. *Structures* 25:347–359. <https://doi.org/10.1016/j.istruc.2020.03.023>
 25. Javidan MM, Kang H, Isobe D, Kim J (2018) Computationally efficient framework for probabilistic collapse analysis of structures under extreme actions. *Eng Struct* 172:440–452. <https://doi.org/10.1016/j.engstruct.2018.06.022>
 26. Song L, Hu H, He J, Chen X, Tu X (2021) Collapse behaviour of a concrete-filled steel tubular column steel beam frame under impact loading. *Adv Mater Sci Eng*. <https://doi.org/10.1155/2021/6637014>
 27. Zhou X, He Y, Xiang S, Zhang Y, Ke K, Wang W (2022) Experimental and numerical studies on structural response of steel garage subjected to vehicular collision. *Structures* 37:933–946. <https://doi.org/10.1016/j.istruc.2022.01.068>
 28. Janfada IS, Sheidaii MR, Kiakojouri F (2023) Comparative analysis of code-based dynamic column removal and impact-induced progressive collapse in steel moment-resisting frames. *Int J Steel Struct* 23(6):1576–1586. <https://doi.org/10.1007/s13296-023-00788-2>
 29. Kiakojouri F, De Biagi V (2024) Catenary mechanism in steel columns under extreme lateral loading: a basis for building progressive collapse analysis. *Dev Built Environ* 20:100556. <https://doi.org/10.1016/j.dibe.2024.100556>
 30. Yi F, Yi W-J, Sun J-M, Zhou Y, Zhang W-X, He Q-F (2024) Experimental study on progressive collapse behavior of frame structures triggered by impact column removal. *Eng Struct* 321:119022. <https://doi.org/10.1016/j.engstruct.2024.119022>
 31. Kukla D, Kozłowski A, Miller B, Ziaja D, Wójcik-Grząba I, Gubernat S (2025) Experimental study of innovative steel beam-to-column joint under impact loading to mitigate progressive collapse. *J Build Eng*. <https://doi.org/10.1016/j.jobe.2025.112018>
 32. Lu Z, Rong K, Zhou Z, Du J (2020) Experimental study on performance of frame structure strengthened with foamed aluminum under debris flow impact. *J Perform Constr Facil* 34(2):04020011. [https://doi.org/10.1061/\(ASCE\)CF.1943-5509.0001403](https://doi.org/10.1061/(ASCE)CF.1943-5509.0001403)
 33. Alam MI, Fawzia S (2015) Numerical studies on cfrp strengthened steel columns under transverse impact. *Compos Struct* 120:428–441. <https://doi.org/10.1016/j.compstruct.2014.10.022>
 34. Kang H, Kim J (2017) Response of a steel column-footing connection subjected to vehicle impact. *Struct Eng Mech* 63(1):125–136. <https://doi.org/10.12989/sem.2017.63.1.125>
 35. Xiang S, He Y, Zhou X (2021) Behaviour and failure modes of steel parking structure column under transverse impact. *Thin-Walled Struct* 167:108163. <https://doi.org/10.1016/j.tws.2021.108163>
 36. Chen C, Zhao Y, Li J (2015) Experimental investigation on the impact performance of concrete-filled frp steel tubes. *J Eng Mech* 141(2):04014112. [https://doi.org/10.1061/\(ASCE\)EM.1943-7889.0000833](https://doi.org/10.1061/(ASCE)EM.1943-7889.0000833)
 37. Kadhim MM, Wu Z, Cunningham LS (2018) Experimental study of cfrp strengthened steel columns subject to lateral impact loads. *Compos Struct* 185:94–104. <https://doi.org/10.1016/j.compstruct.2017.10.089>
 38. Wang W, Wu C, Liu Z, An K, Zeng J-J (2020) Experimental investigation of the hybrid frp-uhpc-steel double-skin tubular columns under lateral impact loading. *J Compos Constr* 24(5):04020041. [https://doi.org/10.1061/\(ASCE\)CC.1943-5614.0001057](https://doi.org/10.1061/(ASCE)CC.1943-5614.0001057)
 39. Minhas A (2024) Seema: Numerical simulation of projectile impact on reinforced concrete structures: a study of slab performance under varying projectile velocities using ansys. *Innov Infrastruct Solut* 9(10):372. <https://doi.org/10.1007/s41062-024-01671-7>
 40. Ferrer B, Ivorra S, Segovia E, Irlés R (2010) Tridimensional modeling of the impact of a vehicle against a metallic parking column at a low speed. *Eng Struct* 32(8):1986–1992. <https://doi.org/10.1016/j.engstruct.2010.02.032>
 41. Zhu A-Z, Xu W, Gao K, Ge H-B, Zhu J-H (2018) Lateral impact response of rectangular hollow and partially concrete-filled steel tubular columns. *Thin-Walled Struct* 130:114–131. <https://doi.org/10.1016/j.tws.2018.05.009>
 42. Aghdamy S, Thambiratnam D, Dhanasekar M (2016) Experimental investigation on lateral impact response of concrete-filled double-skin tube columns using horizontal-impact-testing system. *Exp Mech* 56(7):1133–1153. <https://doi.org/10.1007/s11340-016-0156-z>
 43. Kang H, Kim J (2015) Progressive collapse of steel moment frames subjected to vehicle impact. *J Perform Constr Facil* 29(6):04014172. [https://doi.org/10.1061/\(ASCE\)CF.1943-5509.0000665](https://doi.org/10.1061/(ASCE)CF.1943-5509.0000665)
 44. Kang H, Kim J (2020) Damage mitigation of a steel column subjected to automobile collision using a honeycomb panel. *J Perform Constr Facil* 34(1):04019107. [https://doi.org/10.1061/\(ASCE\)CF.1943-5509.0001394](https://doi.org/10.1061/(ASCE)CF.1943-5509.0001394)
 45. Al-Thairy H, Wang Y (2014) Simplified fe vehicle model for assessing the vulnerability of axially compressed steel columns against vehicle frontal impact. *J Constr Steel Res* 102:190–203. <https://doi.org/10.1016/j.jcsr.2014.07.005>
 46. Santos AF, Santiago A, Latour M, Rizzano G (2020) Robustness analysis of steel frames subjected to vehicle collisions. *Structures* 25:930–942. <https://doi.org/10.1016/j.istruc.2020.03.043>
 47. Xiang S, He Y, Zhou X, Wang W (2021) Continuous twice-impact analysis of steel parking structure columns. *J Constr Steel Res* 187:106989. <https://doi.org/10.1016/j.jcsr.2021.106989>
 48. Zheng L, Wang W-D, Xiao M, Yu Y-Q, Sun H-F (2025) Bionic energy absorbers for parking structural columns against multi-angle vehicle collisions. *J Constr Steel Res* 226:109262. <https://doi.org/10.1016/j.jcsr.2024.109262>
 49. de Mattos LEG, Carneiro JCCB, Beck AT (2025) Risk-based optimum design of a device to simultaneously protect building columns against accidental impact, fire and progressive slab collapse. *Eng Struct* 332:119983. <https://doi.org/10.1016/j.engstruct.2025.119983>
 50. Sadeghi A, Kazemi H, Mehdizadeh K, Jadali F (2022) Fragility analysis of steel moment-resisting frames subjected to impact actions. *J Build Pathol Rehabil* 7(1):1–14. <https://doi.org/10.1007/s41024-022-00165-2>
 51. Nassr AA, Razaqpur AG, Tait MJ, Campidelli M, Foo S (2014) Dynamic response of steel columns subjected to blast loading. *J Struct Eng* 140(7):04014036. [https://doi.org/10.1061/\(ASCE\)ST.1943-541X.0000920](https://doi.org/10.1061/(ASCE)ST.1943-541X.0000920)
 52. Ritchie CB, Packer JA, Seica MV, Zhao X-L (2017) Behavior of steel rectangular hollow sections subject to blast loading. *J Struct Eng* 143(12):04017167. [https://doi.org/10.1061/\(ASCE\)ST.1943-541X.0001922](https://doi.org/10.1061/(ASCE)ST.1943-541X.0001922)
 53. Hadjioannou M, McKay AE, Benschopf PC (2021) Full-scale blast tests on a conventionally designed three-story steel braced frame

- with composite floor slabs. *Vibration* 4(4):865–892. <https://doi.org/10.3390/vibration4040049>
54. Ministero per le infrastrutture: Aggiornamento delle norme tecniche per le costruzioni (in Italian). Supplemento ordinario della Gazzetta Ufficiale della Repubblica Italiana Serie Generale 42 (2018)
 55. Kiakojouri F, Sheidaii M (2019) Numerical analysis of steel i-core sandwich panels subjected to multiple consecutive blast scenarios. *Iran J Sci Technol Trans Civ Eng* 43(Suppl 1):371–382. <https://doi.org/10.1007/s40996-018-0171-7>
 56. Kiakojouri F, Tavakoli HR, Sheidaii MR, De Biagi V (2022) Numerical analysis of all-steel sandwich panel with drilled i-core subjected to air blast scenarios. *Innov Infrastruct Solut* 7(5):320. <https://doi.org/10.1007/s41062-022-00912-x>
 57. Wang J, Wang W, Lehman D, Roeder C (2019) Effects of different steel-concrete composite slabs on rigid steel beam-column connection under a column removal scenario. *J Constr Steel Res* 153:55–70. <https://doi.org/10.1016/j.jcsr.2018.09.025>
 58. Wang J, Wang W (2022) Macromodeling approach and robustness enhancement strategies for steel frame buildings with composite slabs against column loss. *J Struct Eng* 148(1):04021238. [https://doi.org/10.1061/\(ASCE\)ST.1943-541X.0003214](https://doi.org/10.1061/(ASCE)ST.1943-541X.0003214)
 59. Feng D-C, Zhang M-X, Brunesi E, Parisi F, Yu J, Zhou Z (2022) Investigation of 3d effects on dynamic progressive collapse resistance of rc structures considering slabs and infill walls. *J Build Eng*. <https://doi.org/10.1016/j.jobe.2022.104421>
 60. Alrubaidi M, Alhammadi S (2022) Investigation of different infill wall effects on performance of steel frames with shear beam-column connections under progressive collapse. *Latin Am J Solids Struct*. <https://doi.org/10.1590/1679-78256983>
 61. Alrubaidi M, Alhammadi S (2022) Effectiveness of masonry infill walls on steel frames with different beam-column connections under progressive collapse. *Structures* 38:202–224
 62. Kiakojouri F, Sheidaii M, De Biagi V, Chiaia B (2020) Progressive collapse assessment of steel moment-resisting frames using static-and dynamic-incremental analyses. *J Perform Constr Facil* 34(3):04020025. [https://doi.org/10.1061/\(ASCE\)CF.1943-5509.0001425](https://doi.org/10.1061/(ASCE)CF.1943-5509.0001425)
 63. De Biagi V, Marchelli M, Peila D (2020) Reliability analysis and partial safety factors approach for rockfall protection structures. *Eng Struct* 213:110553. <https://doi.org/10.1016/j.engstruct.2020.110553>
 64. Xiang S, He Y, Zhou X (2022) Simplified analytical procedure to calculate the impact behaviour of steel parking-structure columns. *Structures* 46:1938–1954. <https://doi.org/10.1016/j.istruc.2022.11.045>
 65. Xiang S, He Y, Golea T, Denoël V, Demonceau J-F (2024) Simplified methods to predict the robustness of steel parking-structure joints. *J Constr Steel Res* 213:108355. <https://doi.org/10.1016/j.jcsr.2023.108355>
 66. GSA (2013) Alternate path analysis & design guidelines for progressive collapse resistance, Washington, DC
 67. Li W, Gu Y-Z, Han L-H, Zhao X-L, Wang R, Nassirnia M, Heidarpour A (2019) Behaviour of ultra-high strength steel hollow tubes subjected to low velocity lateral impact: experiment and finite element analysis. *Thin-Walled Struct* 134:524–536. <https://doi.org/10.1016/j.tws.2018.10.026>
 68. Yong AC, Lam NT, Menegon SJ (2023) Collision actions on structures. CRC Press, Boca Raton
 69. Yi F, Yi W-J, Sun J-M, Ni J, He Q-F, Zhou Y (2024) On the progressive collapse performance of rc frame structures under impact column removal. *Eng Struct* 307:117926. <https://doi.org/10.1016/j.engstruct.2024.117926>